Shackleton, N.J., Curry, W.B., Richter, C., and Bralower, T.J. (Eds.), 1997
*Proceedings of the Ocean Drilling Program, Scientific Results*, Vol. 154

# 19. PLEISTOCENE VARIATIONS IN DEEP ATLANTIC CIRCULATION AND CALCITE BURIAL BETWEEN 1.2 AND 0.6 MA: A COMBINED DATA-MODEL APPROACH[1]

Peter deMenocal,[2] David Archer,[3] and Peter Leth[4]

**ABSTRACT**

Carbonate percentage and burial flux data for the 1.2–0.6 Ma interval at Ceara Rise Sites 925, 928, and 929 indicate coherent, in-phase variations in carbonate burial, global ice volume (benthic $\delta^{18}O$) and Atlantic deep circulation (benthic $\delta^{13}C$). A time-dependent calcite dissolution model is used to explore the sedimentary signatures of this and other processes. The data and model results are best reconciled if the strong 100-k.y. and 41-k.y. Atlantic carbonate cycles are interpreted in terms of rapid dissolution response signatures related to reduced glacial North Atlantic Deep Water production and associated northward incursion of corrosive Antarctic Bottom Water.

Whereas these Atlantic sediments exhibit in-phase covariation between carbonate burial and deep circulation, Pacific and Indian Ocean carbonate records significantly lag glacial ice volume. Carbonate burial outside the Atlantic basin during glacial intervals is interpreted to be related to enhanced preservation resulting from the temporary increase in mean ocean alkalinity levels (due to Atlantic carbonate dissolution) and the associated 5- to 10-k.y. carbonate ion response time. Based on these results, deep Atlantic circulation changes appear to be the dominant process responsible for the observed Pacific and Indian Ocean glacial-interglacial carbonate deposition patterns.

## INTRODUCTION

Pleistocene changes in deep ocean circulation are now well documented (Boyle and Keigwin, 1982; Oppo and Fairbanks, 1987; Curry et al., 1988; Duplessy et al., 1988; Raymo et al., 1990) and are thought to play a major, active role in regulating glacial-interglacial climate change (Imbrie et al., 1993). A lesser understood element of this phenomenon is the effect of these deep circulation changes on the net burial mass flux of sedimentary calcite. Atlantic sediments accumulating above the lysocline collectively comprise a significant proportion (~50%) of the global sedimentary calcite sink required to balance the riverine alkalinity influx (Milliman, 1993). Although there is abundant evidence that Atlantic dissolution was enhanced during glacial maxima (e.g., Gardner, 1975; Crowley, 1983; Crowley, 1985; Verardo and McIntyre, 1994), the sensitivity of Atlantic sedimentary calcite burial to deep-ocean carbonate chemistry changes has yet to be examined quantitatively.

### Deep Atlantic Hydrography

The northward surface Gulf Stream flow transports accumulated tropical heat and salt to higher latitudes. Subsequent cooling and sinking of this surface water in the Greenland, Iceland, and Norwegian (GIN) Seas produces North Atlantic Deep Water (NADW), which flows southward at depths >2 km and ventilates the deep Atlantic and other ocean basins. In the absence of other factors, NADW formation is perpetuated by linked northward advection, sensible and latent cooling, evaporative salinization, and thermohaline overturn of GIN Seas surface waters. The direct thermal effects of this limb of the global ocean circulation conveyor on western European and Scandinavian climate are significant: the associated Atlantic heat transport poleward of 24°N is 1 PW (petawatt), or roughly 2% of the annual tropical incident radiation (Gill, 1982).

Atlantic deep circulation can be traced also by the subsurface distributions of dissolved nutrients and carbon isotopic compositions of dissolved $\Sigma CO_2$, which trace the mixing of northern-source and southern-source deep-water masses. Because it is formed from well-oxygenated, nutrient-depleted surface waters, NADW is characterized by relatively low initial ("preformed") phosphate and high carbonate ion ($CO_3^=$) concentrations. The $\delta^{13}C$ composition of core NADW water in the deep North Atlantic averages 1.0 ‰. In contrast, Antarctic Bottom Water (AABW) is formed from nutrient-rich surface waters of the Southern Ocean and is distinguished by higher initial nutrient contents and lower carbonate ion concentrations, with mean $\delta^{13}C$ composition near 0.5‰ (Kroopnick, 1985). The shallower southward flow of NADW overrides the deeper northward flow of AABW in the vicinity of the Ceara Rise. The mixing zone between these two end member water masses coincides with the calcite lysocline at ~4100 m (Curry, Shackleton, Richter, et al., 1995). The calcite lysocline shoals from ~4900 m in the North Atlantic to ~3800 m in the South Atlantic due to the increasing proportion of corrosive AABW (Broecker and Takahashi, 1978).

Benthic foraminiferal $\delta^{13}C$ and Cd/Ca data from Atlantic and Southern Ocean cores demonstrate that deep (>2 km) NADW production was dramatically reduced during glacial maxima (Curry et al., 1988; Duplessy et al., 1988; Boyle and Keigwin, 1987; Curry and Lohmann, 1990; Charles and Fairbanks, 1992), whereas upper NADW (<2 km) was enhanced (Oppo et al., 1995; Oppo and Lehman, 1993; Oppo and Fairbanks, 1990; deMenocal et al., 1992). North Atlantic sea-surface temperatures (SSTs) were also greatly reduced during these glacial intervals (Raymo et al., 1990), suggesting a reduction in the efficiency of the thermohaline conveyor limb that forms NADW. Although the precise mechanism linking ocean circulation and climate change remains elusive (see Imbrie et al., 1993; Curry, 1996), the thermal effects of changes in ocean circulation are readily apparent from the marine sediment record. The glacial North Atlantic was cooler by ~10°–12°C (CLIMAP Project Members, 1981; Ruddiman et al., 1986). Ocean modeling studies indicate that

[1]Shackleton, N.J., Curry, W.B., Richter, C., and Bralower, T.J. (Eds.), 1997. *Proc. ODP, Sci. Results,* 154: College Station, TX (Ocean Drilling Program).
[2]Lamont-Doherty Earth Observatory, Palisades, NY 10964 U.S.A.
peter@ldeo.columbia.edu
[3]The University of Chicago, Chicago, IL 60637, U.S.A.
[4]Pomona College, Claremont, CA 91711-6339, U.S.A.

NADW shutdown alone cools North Atlantic SSTs by 6°–8°C (e.g., Rahmsdorf, 1995).

Changes in NADW production present significant ocean paleochemical implications as well. During glacial periods when NADW production was reduced, the deep mixing zone between NADW and AABW moved northward from its current equatorial position into the high-latitude North Atlantic (Raymo et al., 1990). Carbonate sediments accumulated during these intervals are characterized by intense dissolution, abundant foraminifer fragmentation, and low carbonate percentage and mass accumulation rates (Gardner, 1975; Verardo and McIntyre, 1994; Curry and Lohmann, 1986, 1990; Balsam, 1983). During some glacial maxima of the Pliocene–Pleistocene, North Atlantic $\delta^{13}C$ values were indistinguishable from deep Pacific values, documenting dramatic incursions of nutrient-rich, highly corrosive AABW into the carbonate-rich basins of the North Atlantic (Oppo and Fairbanks, 1987; Raymo et al., 1990; Oppo and Lehman, 1993). In that the Atlantic surface sediments collectively comprise a massive reservoir of sedimentary carbonate, these past glacial incursions of undersaturated AABW over these sediments and resulting dissolution imply significant increases in mean ocean alkalinity that must have been balanced by net preservation and burial in other ocean basins within the 5- to 10-k.y. oceanic [$CO_3^=$] response time**.**

## Strategy

We employ a combined data-model approach to quantify the covariability between deep Atlantic circulation change and net sedimentary carbonate burial. The goal of the present study is to document this phenomenon using the unique depth-transect sites recovered during Leg 154 and to define the coupling between Atlantic deep circulation change and equatorial Atlantic carbonate burial over an interval of strong NADW production variability. Here, we use the carbon isotopic composition of benthic foraminifers to reconstruct past variations in the relative contribution of NADW to the deep waters that bathed these tropical western Atlantic sites between 1.2 and 0.6 Ma. This interval was selected because it is characterized by rapid and high-amplitude fluctuations in NADW production (Fig. 1; Raymo et al., 1990). Linkages between changes in deep-water circulation and calcite burial are examined by comparing the paleocirculation to calcium carbonate percentage and flux data from three Ceara Rise sites spanning a depth range of 3000–4300 m. Finally, a time-dependent version of the Archer (1991) sedimentary calcite dissolution model is used to conduct a series of experiments that examine the differing sedimentary signatures associated with isolated variations in calcite rain rate, terrigenous rain rate, and deep, circulation-driven dissolution changes for a series of hypothetical sediment cores along a bathymetric slope. The core data and model results are then merged to define the mechanisms regulating carbonate burial on the Ceara Rise and to interpret these Atlantic carbonate burial cycles within the context of Pacific and Indian Ocean carbonate accumulation records.

## METHODS AND AGE MODELS

The 1.2–0.6 Ma interval of Sites 925 (4°12.2N, 43°29.3W, 3042 m water depth), 928 (5°27.3N, 43°44.9W, 4011 m), and 929 (5°58.6N, 43°44.4W, 4358 m) were sampled from their respective composite sections at 10-cm intervals (Curry, Shackleton, Richter, et al., 1995). These sites were selected because they represent the shallowest and two deepest sites in the depth transect (Fig. 2). Site 925 is presently within the core of NADW flow with an average $\delta^{13}C$ composition of ~1‰ and a $\Delta CO_3^=$ supersaturation value of +35 µm (Oppo and Fairbanks, 1987; Curry, 1996). Site 928 is presently located near the calcite saturation ($\Delta CO_3^= = 0$) horizon at the NADW/AABW mixing horizon. Site 929 is presently within the colder, lower salinity AABW flow with an average $\delta^{13}C$ composition of ~0.5‰ and a

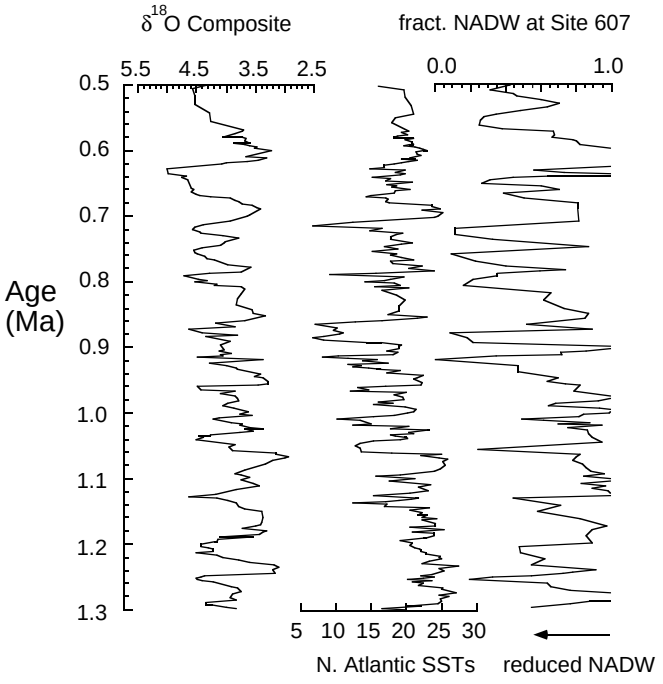


Figure 1. The percent NADW record calculated from the Site 607 carbon isotopic record (41°N; Raymo et al., 1990). Positive values indicate efficient NADW ventilation of the deep Atlantic at 41°N, whereas values approaching zero indicate reduced NADW ventilation.

$\Delta CO_3^=$ undersaturation value of –5 µm (Oppo and Fairbanks, 1987; Curry, 1996).

Based on average sedimentation rates near 4–5 cm/k.y. (Curry, Shackleton, Richter, et al., 1995) this sample interval is roughly equivalent to a 2.5-k.y. time interval. All samples were freeze dried, ground, and analyzed for calcium carbonate percent using the carbonate Coulometer. Analytical precision (1 σ) calculated from several hundred replicated analyses of two internal standards using the Lamont Doherty Earth Observatory instrument was 0.5 wt%.

Samples from Sites 925 and 929 were shaken 2 hr in a 4% calgon solution and then washed with deionized water through a 64-µm sieve; the coarse fraction was dried at 50°C and weighed. Three taxa of benthic foraminifers were picked for analysis from the dry-sieved >150-µm fraction: *Cibicides wuellerstorfi,* mixed *Cibicides* spp., and *Nuttallides umbonifera*. At some levels in Site 925, *Uvigerina pygmaea* was also picked due to the complete absence of the other three preferred taxa. An average of 12 specimens was picked for analysis for each sample. Some samples yielded as few as three to five specimens, which were also analyzed. All samples were analyzed on the Woods Hole Oceanographic Institution Finnegan MAT252 mass spectrometer with the Kiel automated carbonate preparation device. Samples were not roasted prior to analysis. The external precision of the isotopic analyses was ±0.03‰ for $\delta^{13}C$ and ±0.07‰ for $\delta^{18}O$ based on more than 1200 measurements of NBS19 standard.

Some samples of Site 929 contained no benthic (or other) foraminifers due to extreme dissolution. One particularly long interval occurred between 30.87 and 31.57 meters composite depth (mcd; 0.81–0.79 Ma) in Site 929 where no benthic foraminifers were found in the >64-µm fraction and the planktonic foraminifers within this interval were extremely fragmented. This interval corresponds to a severe reduction in NADW production as monitored by the benthic isotope record at Site 607 (Fig. 1; Raymo et al., 1990). The benthic isotope record at Site 925 was less affected by these extreme dissolution

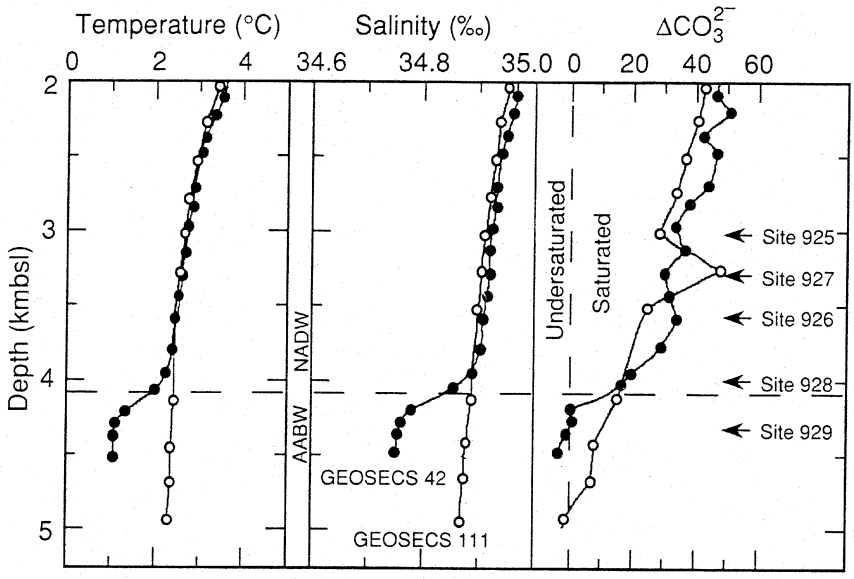


Figure 2. Water depth locations for Sites 925–929 and regional western tropical Atlantic hydrographic data (Curry, Shackleton, Richter, et al., 1995).

events, but analyses for the 1.1–1.2 Ma interval are not yet completed.

All isotopic data have been corrected to seawater values. A correction of +0.64‰ has been added to the $\delta^{18}O$ values of *Cibicides wuellerstorfi* and mixed *Cibicides wuellerstorfi* (Shackleton, 1974). Based on paired *Cibicides* and *Nuttallides umbonifera* analyses from Keigwin and Lehmann (1994), the $\delta^{18}O$ and $\delta^{13}C$ values of *Nuttallides umbonifera* were adjusted by +0.2‰ and −0.2‰, respectively. The few *Uvigerina pygmaea* analyses were corrected by adding +0.90‰ to the measured $\delta^{13}C$ values (Duplessy et al., 1984).

All core data have been transformed to age using the tuned magnetic susceptibility age model presented in Bickert et al. (Chapter 16, this volume) to assure compatibility with other datasets presented in this volume. The validity of this age model was checked by continuously-tuning the Site 925 and 929 oxygen isotopic stratigraphies to the Site 677 oxygen isotopic time scale.

Carbonate and terrigenous mass flux records were calculated from the relative proportion of carbonate and non-carbonate sediment at each level at Sites 925, 928, and 929, and the interval sedimentation rates were derived from the age models. Physical properties and continuous Gamma-ray Attenuation Porosity Evaluator (GRAPE) bulk-density data demonstrate that sediment bulk densities were largely invariant either between sites or within sites or as a function of carbonate percentage over this time interval, in agreement with detailed piston core data from the region (Curry and Lohmann, 1990). An average dry bulk density was determined from shipboard data for the 1.2–0.6 Ma interval at each site and a mean value of 0.95 g/cm$^3$ was calculated; this average value was used for all sediment flux calculations.

All carbonate and benthic isotopic data presented in this paper (depth and time series) can be found in the CD-ROM enclosed with this volume.

## DATA RESULTS

Over the 1.2–0.6 Ma interval considered in this study, glacial intervals at all sites have lower carbonate percentages and accumulation rates and lower coarse (>64 µm) fraction percentages than interglacial sediments (Fig. 4). The carbonate percentage, accumulation rate, and coarse fraction data closely covary (Fig. 3) and in-phase with each other at the dominant 100-k.y. and 41-k.y. periods of variation (Table 1). The close, in-phase covariance between carbonate percentage and accumulation rate data demonstrate that carbonate percentage data at all sites reflect real variations in carbonate burial rates (Figs. 3, 4) rather than dilution effects related to variations in noncarbonate sediment supply. Furthermore, these carbonate percentage, accumulation rate, and coarse fraction records are coherent and in-phase with the Site 929 benthic $\delta^{13}C$ record at the dominant 100-k.y. and 41-k.y. periods (Table 1). As expanded upon in the following paragraphs, these results collectively indicate that the primary underlying cause of the Ceara Rise carbonate cycles has been variable carbonate dissolution due to changes in deep Atlantic circulation.

### Carbonate Percent, Accumulation Rate, and Coarse Fraction Data

The average range of glacial-interglacial carbonate fluctuations over the 1.2- to 0.6-Ma interval at each site varies with an approximate amplitude of 50 wt% carbonate (Fig. 4). The shallowest Site 925 carbonate record ranges from 19% to 70%, the middle depth sites 928 ranges from 2% to 61%, and the deepest Site 929 ranges from 0% to 54% over the 1.2- to 0.6-Ma interval (Fig. 3). The highest carbonate values for the shallowest site, Site 925, only attain ~70% due to significant contributions of terrigenous sediment from Amazon basin drainage that enhance sedimentation rates on the Ceara Rise (Curry, 1996).

Shallow-to-deep (Site 925 minus Site 929) carbonate percentage and accumulation rate difference calculations indicate that the tropical western Atlantic lysocline thickness has not varied appreciably in response to the glacial-interglacial changes in deep-water circulation over this 1.2- to 0.6-Ma interval (Fig. 5). Whereas the lysocline position appears to have oscillated over a considerable bathymetric range (as evidenced by the dramatic, synchronous changes in carbonate values at all sites), the thickness of the transition zone (as defined by the shallow-to-deep range of carbonate values over glacial and interglacial intervals [e.g., Farrell and Prell, 1989]) appears to have been relatively constant. In essence, the carbonate percentage and accumulation rate records for the different sites track each other with relatively constant offsets related to water depth (Fig. 4). The Site 925 and 928 carbonate records were correlated into the Site 929 carbonate record using a series of linear interpolation tiepoints to optimally align all carbonate records for the difference calculations. All records

**Table 1. Phase relationships (in degrees) between carbonate percentage, accumulation rate, coarse fraction percent, and isotopic indices of ice volume (Site 929 $\delta^{18}O$) and Atlantic deep circulation (Site 929 $\delta^{13}C$).**

| | 100 k.y. | 41 k.y. | 23 k.y. | 19 k.y. |
|---|---|---|---|---|
| Core data, Site 929 | | | | |
| $-\delta^{18}O$ vs. $\delta^{13}C$ | −17° ± 25 | −7° ± 23 | 60° ± 22 | — |
| $-\delta^{18}O$ vs. $CaCO_3$% | −44° ± 14 | −19° ± 22 | 26° ± 24 | 65° ± 25 |
| $-\delta^{18}O$ vs. $CaCO_3$ acc. rate | — | −13° ± 20 | 26° ± 26 | 65° ± 24 |
| $\delta^{18}C$ vs. Site 929 $CaCO_3$ | −25° ± 24 | −10° ± 21 | −40° ± 24 | — |
| $CaCO_3$ vs. coarse fraction | −1° ± 14 | −6° ± 7 | −9° ± 11 | −1° ± 13 |
| Model results | | | | |
| Forcing signal vs. model $CaCO_3$% ("Dissolution" experiment) | 12° ± 7 | 27° ± 5 | — | — |
| Forcing signal vs. model $CaCO_3$ acc. rate ("Dissolution" experiment) | 2° ± 3 | 6° ± 2 | — | — |

Notes: All results were calculated using the Blackman-Tukey method (Blackman and Tukey, 1958) for the 1.2–0.6 Ma interval using files interpolated at 3 k.y.; listed results are significant at the 95% confidence interval. Negative values indicate that the first record lags (occurs chronologically after) the second record; positive values mean the second record lags the first.

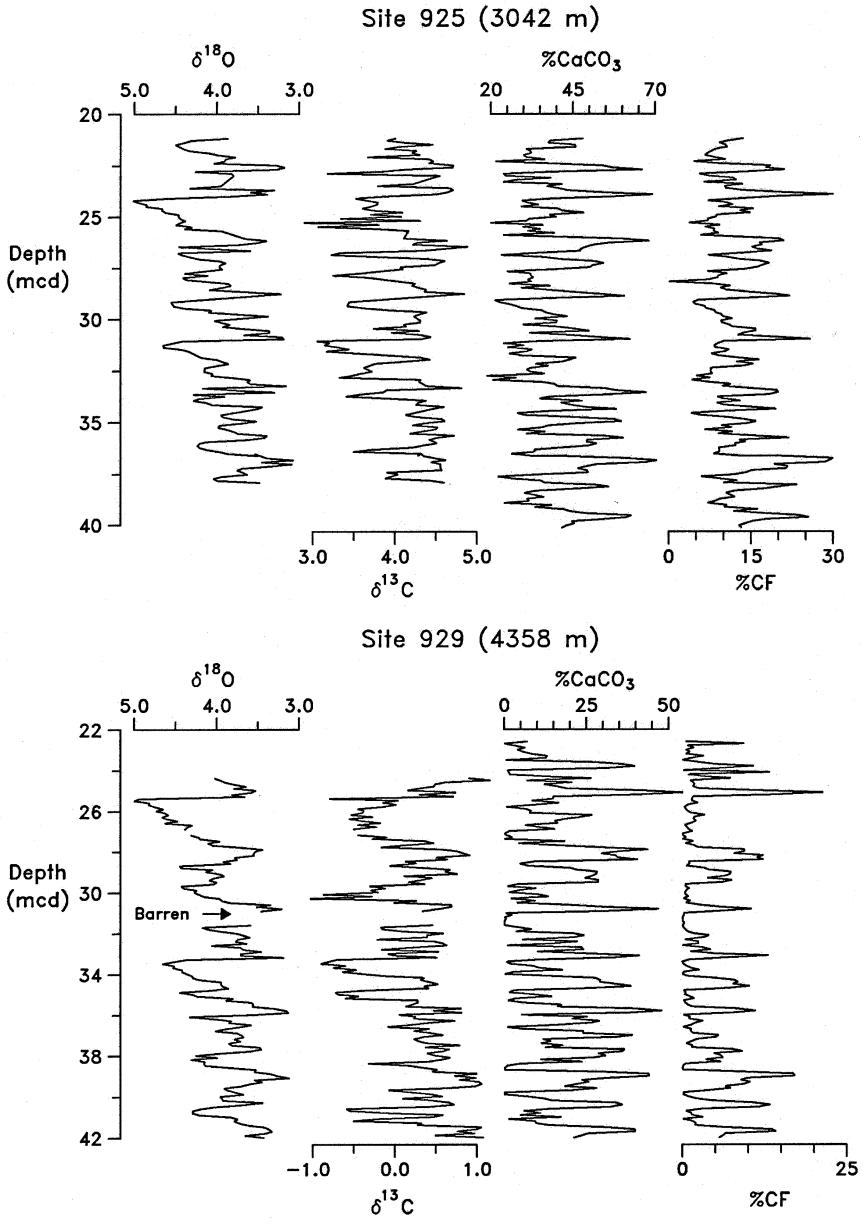


Figure 3. Benthic $\delta^{18}O$ and $\delta^{13}C$ values (mainly based on *C. wuellerstorfi* analyses) and carbonate percentage and coarse fraction (CF; >64 µm) data for Sites 925 and 929. All isotopic data have been corrected to seawater values (see text). All samples were taken from the shipboard composite sections developed for these sites (see Curry, Shackleton, Richter, et al., 1995).

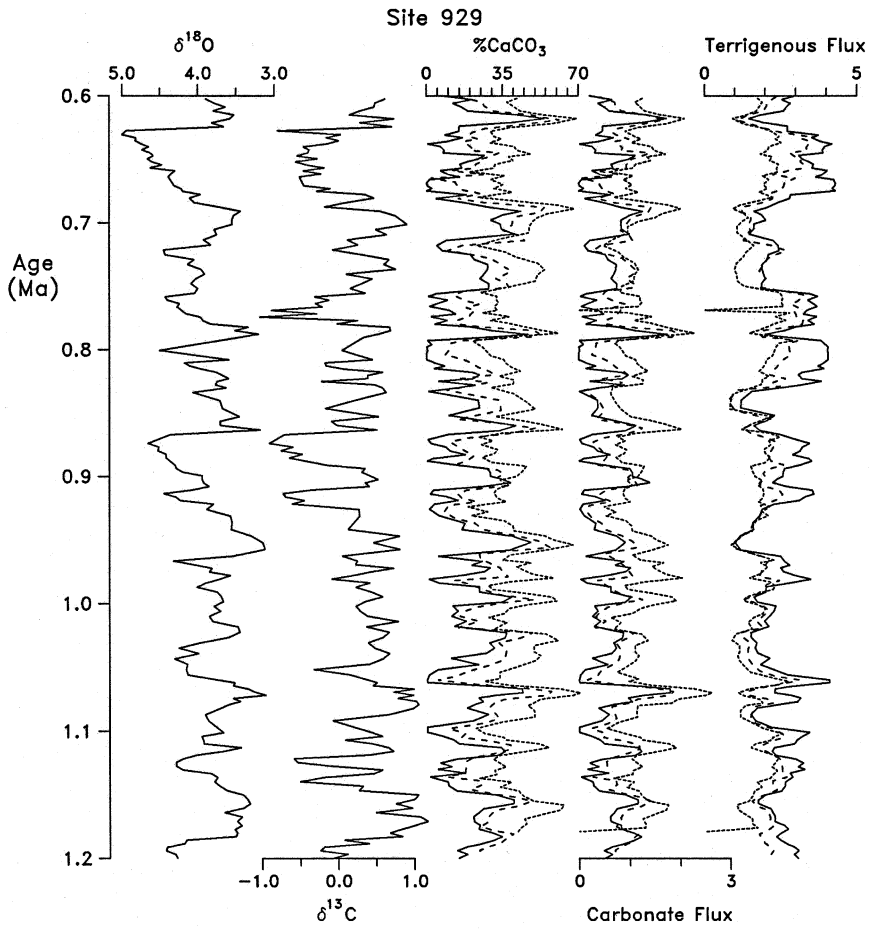


Figure 4. Benthic isotopic data for Site 929 (adjusted to seawater values) and carbonate percentage, flux, and terrigenous flux data for Sites 925 (short dash), 928 (long dashed line), and 929 (unbroken line). Age models at all sites were calculated using the Bickert et al. (Chapter 16, this volume) discrete (not continuous) correlations into a lagged orbital isolation target curve. Accumulation rate data were calculated using interval sedimentation rate data and component abundances, assuming a mean dry bulk-density value of 0.95 g/cm$^2$ at all sites.

were then interpolated at a 3-k.y time step, and the shallow-to-deepest (Site 925 minus Site 929) and intermediate-to-deepest (Site 928 minus Site 929) differences in carbonate percent and mass accumulation rate were calculated. These data (Fig. 5) demonstrate that despite relatively large amplitude glacial-interglacial variations in carbonate percentages and accumulation rates at all sites (Figs. 3, 4), associated variations in the amount carbonate buried at shallow vs. deep sites were low. Low squared correlation coefficients between the Site 929 carbonate percentages (accumulation rates) vs. the Site 925 minus Site 929 percentage (accumulation rate) differences confirm the lack of systematic lysocline thickness changes associated with the carbonate cycles (respectively, $r^2 = 0.21$ [0.01]).

## Frequency-Domain Analyses

Power-spectral and cross-spectral analyses demonstrate that the dominant periods of carbonate variability occur at 41 k.y. and 100 k.y. (Fig. 6), and that variations in carbonate percent, accumulation rate, and coarse fraction are coherent and in-phase with changes in $\delta^{13}C$ (deep ocean circulation) and $\delta^{18}O$ (global ice volume; Table 1). The carbonate records have a lesser amount of variation at the precessional bands (23–19 k.y.), but they appear to lead both $\delta^{13}C$ and $\delta^{18}O$ by several thousand years although the associated phase error is high (Table 1). We used the Blackman-Tukey method of spectral estimation (Blackman and Tukey, 1958), using a 3-k.y. time step with one-third lag and reported coherences and phases that exceed the 95% confidence level.

The Site 929 benthic $\delta^{13}C$ record varied coherently and out of phase with benthic $\delta^{18}O$ at the dominant 100-k.y. and 41-k.y. orbital bands (100-k.y. band, 163° ± 25°; 41-k.y. band, 173° ± 23°). At the subordinate 23-k.y. precessional period, benthic $\delta^{13}C$ leads $\delta^{18}O$ significantly (−120° ± 22°). Curry (1996) reported phase results from latest Pleistocene benthic isotope data from the Ceara Rise, which indicated that benthic $\delta^{13}C$ leads $\delta^{18}O$ at the 100-k.y. and 41-k.y. periods, however the associated 80% confidence-level error for the 41-k.y. phase exceeded the apparent lead.

Power spectra of the carbonate percentage and accumulation rate records indicate that the amplitude of the dominant 41-k.y. period of variation varies with water depth (Fig. 6). For the carbonate percentage records, the deepest site (Site 929) has the highest amplitude variations whereas the shallowest site has the lowest amplitude variations (Site 925). This relationship reverses when the carbonate accumulation rate data are considered. The shallow site (925) carbonate flux record exhibits the highest amplitude fluctuations whereas the deepest site (929) has lowest amplitude variations. The significance of these results will become apparent when the model results are discussed; the analytical carbonate percent and flux data can be used to define the origins of the carbonate variations.

## CALCITE DISSOLUTION MODEL EXPERIMENTS

Three model experiments were conducted to explore the sedimentary signatures associated with three end-member scenarios that may have affected carbonate deposition on the Ceara Rise: carbonate rain rate changes (“Production” experiment), deep-water circulation changes (“Dissolution” experiment), and terrigenous supply changes (“Dilution” experiment). We use a time-dependent version of the Ar-

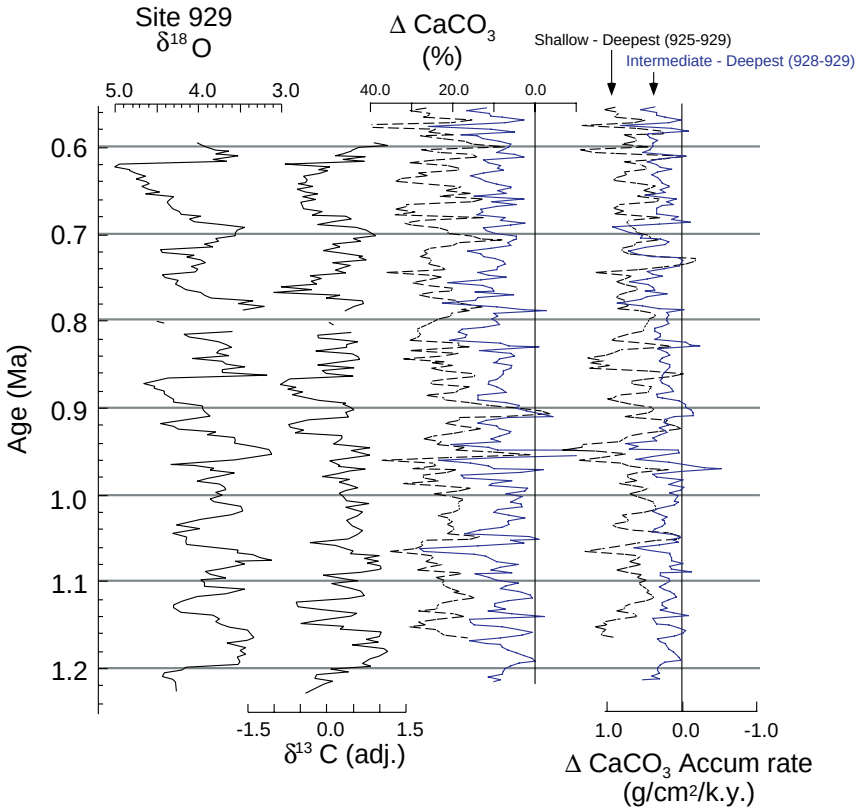


Figure 5. Benthic isotope time series at Site 929 shown adjacent to the between-site $CaCO_3$ percent and $CaCO_3$ accumulation rate differences for the 1.2–0.6 Ma interval. Carbonate percent records were optimally aligned (to adjust for slight time scale errors), the data were interpolated at 3 k.y. intervals, and the carbonate percent and accumulation rate differences were computed between Sites 925–929 (shallowest–deepest) and 928–929 (intermediate–deepest). The lack of covariation between the carbonate percent and the percent differences between sites separated by ~1300 m water depth suggests that the Atlantic lysocline thickness has not changed markedly over this interval. Squared correlation coefficients between the Site 929 carbonate percentages (accumulation rates) vs. the Site 925–929 differenced percentage (accumulation rate) records were low ($r^2 = 0.21$ [0.01]), suggesting that there has been no systematic change in the lysocline thickness associated with the evident vertical migrations of the calcite lysocline.

cher (1991) calcite dissolution model, which calculates equilibrium calcite concentration and accumulation rate values for a region with known bottom-water chemistry, carbonate, non-carbonate, and organic carbon rain rates. Aside from the depth-dependent pressure and temperature controls on carbonate ion concentrations, the model also calculates calcite dissolution due to organic carbon respiration (see model description below; Archer, 1991). The model was adapted to calculate carbonate/non-carbonate percentages and burial fluxes for a series of hypothetical "cores" along a 2.5-km rise structure where the steady-state saturation horizon is set at 1.25 km (Fig. 7). Carbonate and non-carbonate model rain rates were set to mean values determined for Ceara Rise cores (4 g/cm$^2$/k.y. and 0.4 g/cm$^2$/k.y., respectively).

The three end-member model simulations are summarized below. In each case, only one prescribed boundary condition change was imposed using a smoothed benthic (Site 607) $\delta^{18}O$ record (Fig. 7), which was then scaled to match the mean value and desired range of the forcing boundary condition signal.

1. "Production" experiment. The mean $CaCO_3$ rain rate of 4 g/cm$^2$/k.y. was varied by ±50%, and the non-carbonate rain rates and the position of the saturation horizon were held constant.

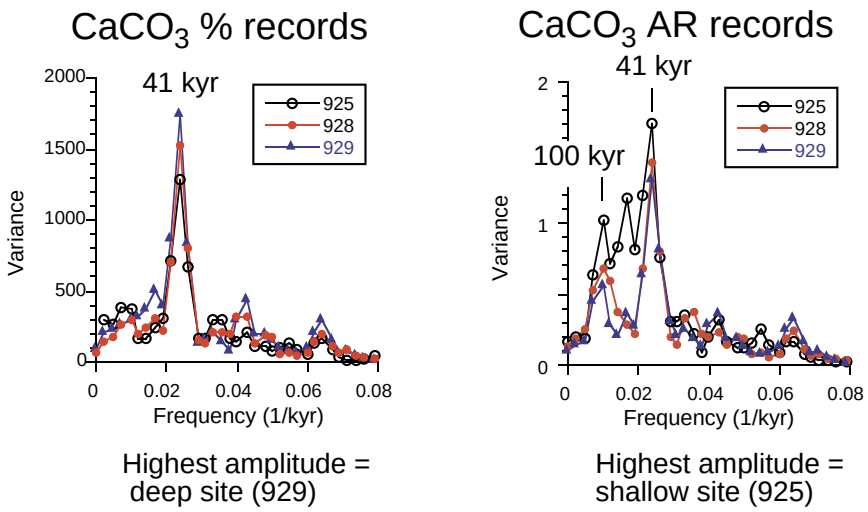


Figure 6. Power spectra of carbonate percentage and accumulation rate (AR) records at Sites 925, 928, and 929. For the carbonate percentage records, the highest amplitude variations occur in the deepest site, Site 929, whereas for the carbonate accumulation rate data the highest amplitude occurs in the shallowest site, Site 925.

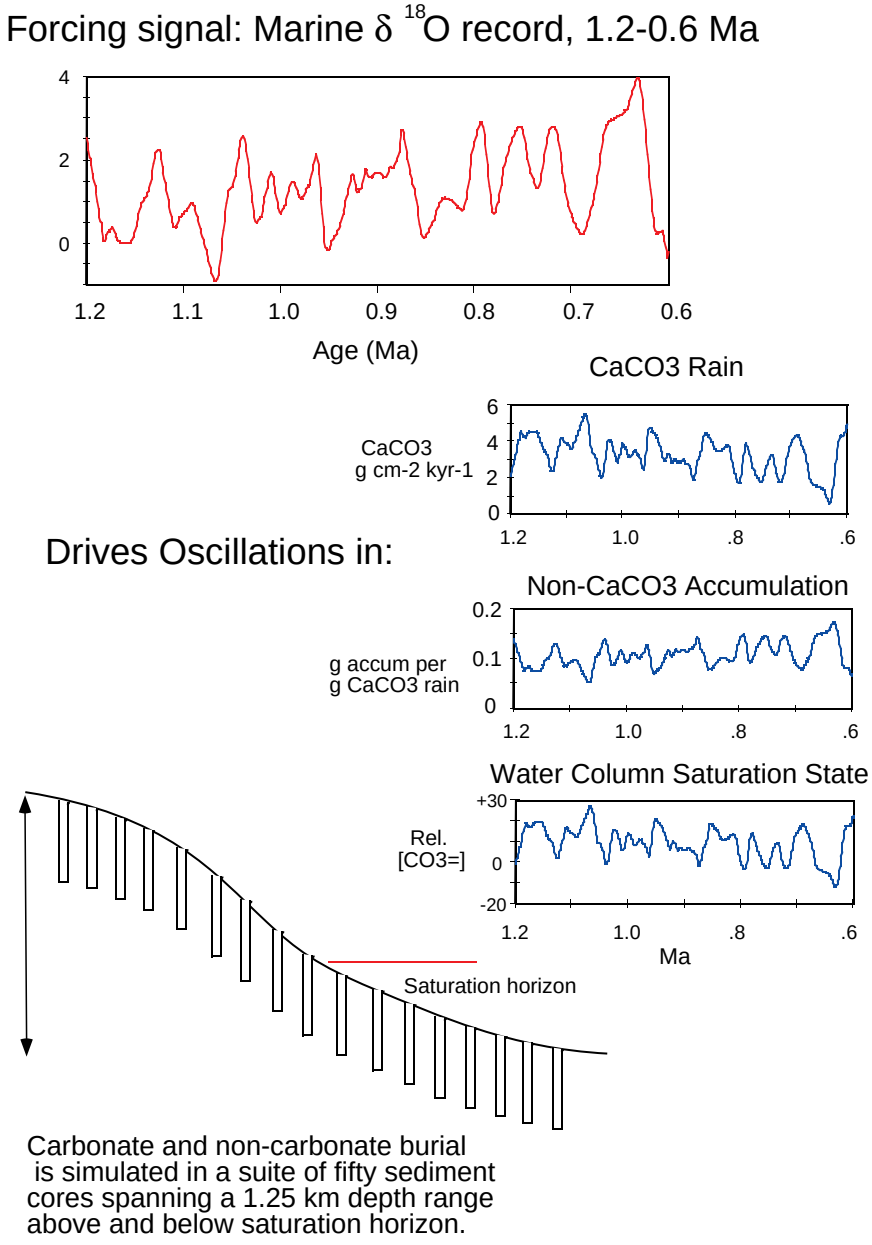


Figure 7. Schematic diagram of the Archer (1991) time-dependent calcite dissolution model. The model was perturbed in three separate experiments to study the sedimentary signatures of changes in carbonate rain rate (Production), variable deep ocean [$\Delta CO_3^=$] (Dissolution), and variable terrigenous supply (Dilution). The model was used to calculate the equilibrium calcite concentration for a series of 50 sediment "cores" along a hypothetical bathymetric gradient (±1.25 km around the control saturation horizon) based on prescribed carbonate and non-carbonate rain rates and the deep ocean carbonate chemistry of the overlying waters. See Archer (1991) for model description and text for experimental design.

Organic carbon flux to the seafloor covaries with carbonate rain rates in modern rain rate ratios (Archer, 1991). This experiment was designed to simulate changes in surface ocean carbonate production.

2. "Dissolution" experiment. The [$\Delta CO_3^=$] concentration (relative to calcite saturation) of deep waters flowing over the shallowest level in the model was varied between +30 µmol and –10 µmol, and the carbonate and non-carbonate rain rates were held constant. The [$\Delta CO_3^=$] range is roughly equivalent the saturation contrast between source NADW waters and the deep equatorial Pacific (Broecker and Takahashi, 1978). This experiment was designed to test the effects of changes in deep-water chemistry tied to deep circulation changes.
3. "Dilution" experiment. The mean non-carbonate (terrigenous) rain rate (0.4 g/cm²/k.y.) was varied by ±50%, and the carbonate rain rates and the position of the saturation horizon were held constant. This experiment was designed to simulate glacial-interglacial variations in Amazon basin terrigenous supply.

## Model Description

The calcite dissolution model is based on the diffusion and reaction of the carbonate buffer species ($CO_2$, $HCO_3^-$, and $CO_3^=$) within the sediment pore water. The model was developed for the interpretation of in situ pore-water micro pH electrode data (Archer, 1989). Emerson and Archer (1992) used the model to predict the depth dependence of calcite in the deep sea. Subsequently, a numerical improvement allowed analysis of the model behavior and comparison with oceanic data in much greater detail. By assuming that the calcite concentration and the sediment pore water are in steady state, the model is able to reproduce the depth dependence of the calcite concentration, within the available constraints of sediment trap, pore-water, and sediment accumulation data.

The time-dependent implementation of the model assumes that the pore-water chemistry remains in steady state at all times (the relaxation time for the pore water in the mixed layer of real sediments is on the order of 1000 hr). The pore-water chemistry at any given

time is determined by the solid chemistry and the surface boundary condition (the chemistry of the overlying water). Also, we assumed that the organic carbon distribution remains in steady state (which relaxes in order 100 yr, based on unpublished numerical experiments). The non-organic sediment is assumed to consist of calcite and a refractory phase (clay), while opal is neglected. The calcite and clay are assumed to be well mixed at all times; both are diluted somewhat near the surface by organic carbon. The isotopic signature of the calcite is also assumed to be well mixed in the mixed layer.

At each time step (which varies from 50 to 500 yr), calcite and clay are added to the mixed layer by sediment rain, and the steady state profiles of pore-water solutes and solid organic carbon are calculated. The calcite concentration and oxygen isotopic ratio of the mixed layer is determined by weighted average of the new and old mixed-layer material. Burial of clay and $CaCO_3$ is computed by difference, to balance the mass flux. The calcite concentration and isotopic signature of the buried material are taken to be the mixed-layer values at that time. The "buried" material is stored in an array of specified mass, calcite concentration, isotopic signature, and porosity (calculated as a function of calcite concentration).

When the mass rain rate is less than the total mass reaction rate, "chemical erosion" occurs. In this case, the material at the top of the buried sediment array is entrained into the mixed layer, and its chemistry and isotopic values are averaged into the mixed layer. When the mass of a parcel of sediment is completely depleted, material from the box below is used, such that total volume in the sediment mixed layer is conserved. The model was checked by running experiments that included both erosional and depositional phases and by verifying the conservation of total mass, calcite, and $\delta^{18}O$. Using initial calibration data, the model successfully calculates the carbonate/non-carbonate percentage and flux value means and ranges that are observed in Ceara Rise cores.

## EXPERIMENT RESULTS

The calculated carbonate percentage and accumulation rate data for the suite of simulated cores along this simulated rise are shown in Figures 8 and 9. The effects of the different boundary conditions on carbonate burial with water depth can be quantified by considering how the amplitude of the resulting carbonate percentage and flux records vary with water depth. Power-spectral amplitudes were calculated for each series of cores in each experiment, and the results are presented as three-dimensional (frequency–spectral density–water depth) power-spectral diagrams in Figure 10.

In the Production experiment, the deepest cores exhibit the highest amplitude variations in carbonate percentage, because they are below the calcite saturation horizon; changes in calcite rain to the deepest sites are amplified by the variable residence time of calcite in the sediment mixed layer and this signal is damped with decreasing water depth (Figs. 8–10). This situation reverses itself when the carbonate accumulation rate data are examined. Carbonate flux amplitudes are always highest in the shallowest cores because they are best able to preserve the full amplitude of the rain rate flux signal.

A similar, though slightly different result is observed in the Dissolution experiment. Highest calcite percentage amplitudes (Figs. 8–10) are detected for the deepest sites, which are subjected to the highest degrees of undersaturation due to the imposed $[\Delta CO_3^{=}]$ changes. Like the previous experiment, this situation reverses itself when the carbonate flux data are considered. Here, the highest amplitude carbonate flux records are those just above the lysocline, whereas flux amplitudes are diminished in deep, sublysoclinal cores. The highest amplitude response in both the carbonate percent and flux records is detected for cores at the lysocline level.

Cross-spectral analysis between the Dissolution model and the calculated carbonate burial flux data (Table 1) indicates coherent and in-phase covariability between the dissolution forcing and calcite burial response. The model $CaCO_3$ percent data lag the forcing signal by ~3–4 k.y. at the 100-k.y. and 41-k.y orbital bands due to the way that the model calculates carbonate percent. Changes in calcite dissolution affect the residence time of calcite in the sediment mixed layer, which takes some time to adjust (3–4 k.y.), whereas calcite flux changes (the instantaneous difference between calcite rain and dissolution) are calculated explicitly by the model.

The Dilution experiment produced very contrasting results. Highest amplitude carbonate percentage variations occur in the shallowest cores, because these have the highest carbonate preservation and are most readily affected by terrigenous dilution. Since carbonate burial flux is only directly affected by water-depth solution effects on $[\Delta CO_3^{=}]$, the carbonate flux variations have very low amplitude at all depths (Fig. 9). Spectral amplitudes were rescaled in Figure 10 to show carbonate flux amplitude variability due to organic carbon respiration.

## DISCUSSION

### Comparison of Core Data and Model Results

The core data and model results indicate that the observed carbonate percent and flux data at the Ceara Rise Sites 925, 928, and 929 can be attributed to changes in calcite dissolution due to glacial-interglacial changes in deep Atlantic circulation. The core data indicate that carbonate percent and burial rates vary coherently and in-phase with benthic $\delta^{18}O$ (ice volume) and $\delta^{13}C$ (deep Atlantic circulation). The core carbonate percentage and flux records also exhibit water-depth-dependent variations in signal amplitude that the model simulations indicate can only be explained in terms of changes either in deep circulation or carbonate productivity. As described below, the Site 929 benthic isotope data indicate dramatic reductions in NADW production coincident with the carbonate percentage and flux minima. The data and model results demonstrate that the Ceara Rise carbonate records cannot be attributed to dilution by variable quantities of terrigenous sediment supply from the Amazon basin.

### Percent NADW Calculation for Site 929

The carbon isotopic record at Site 929 (4300 m) nominally reflects the dual influences of global mean $\delta^{13}C$ changes and regional changes in deep circulation. To isolate the deep circulation component the Site 929 $\delta^{13}C$ must be scaled in terms of relative changes in the initial $\delta^{13}C$ composition of NADW and the $\delta^{13}C$ composition of the deep Pacific (e.g., Oppo and Fairbanks, 1987; Raymo et al., 1990; Mix et al., 1995). To monitor the initial $\delta^{13}C$ composition of NADW formation waters, we selected the benthic isotope record from Site 552A in the North Atlantic (56°N, 23°W, 2301 m; Shackleton et al., 1984). This record is comprised mainly of analyses on *Cibicides wuellerstorfi*, and although it is a relatively low-resolution record ($\Delta t$ = 5 k.y.) and it is not ideally situated to monitor initial NADW $\delta^{13}C$ composition (deMenocal et al., 1992; Mix et al., 1995), it is presently the only suitable record available for this end member. To monitor changes in deep Pacific $\delta^{13}C$ composition, we selected the equatorial Pacific Site 849 (0°N, 110°W, 3851 m; Mix et al., 1995) which is a detailed record mainly comprised of analyses of *C. wuellerstorfi*. All isotopic data have been converted to seawater values (Fig. 11).

Fractional NADW contribution to the water chemistry at Site 929 is calculated from the seawater-corrected carbon isotopic data using the following relation (Oppo and Fairbanks, 1987):

$$NADW_{929} = (\delta^{13}C_{929} - \delta^{13}C_{849}) / (\delta^{13}C_{552A} - \delta^{13}C_{849}).$$

Based on coretop $\delta^{13}C$ data from these sites, the calculated fractional NADW value is 0.33 (33%). While this equation produces a useful

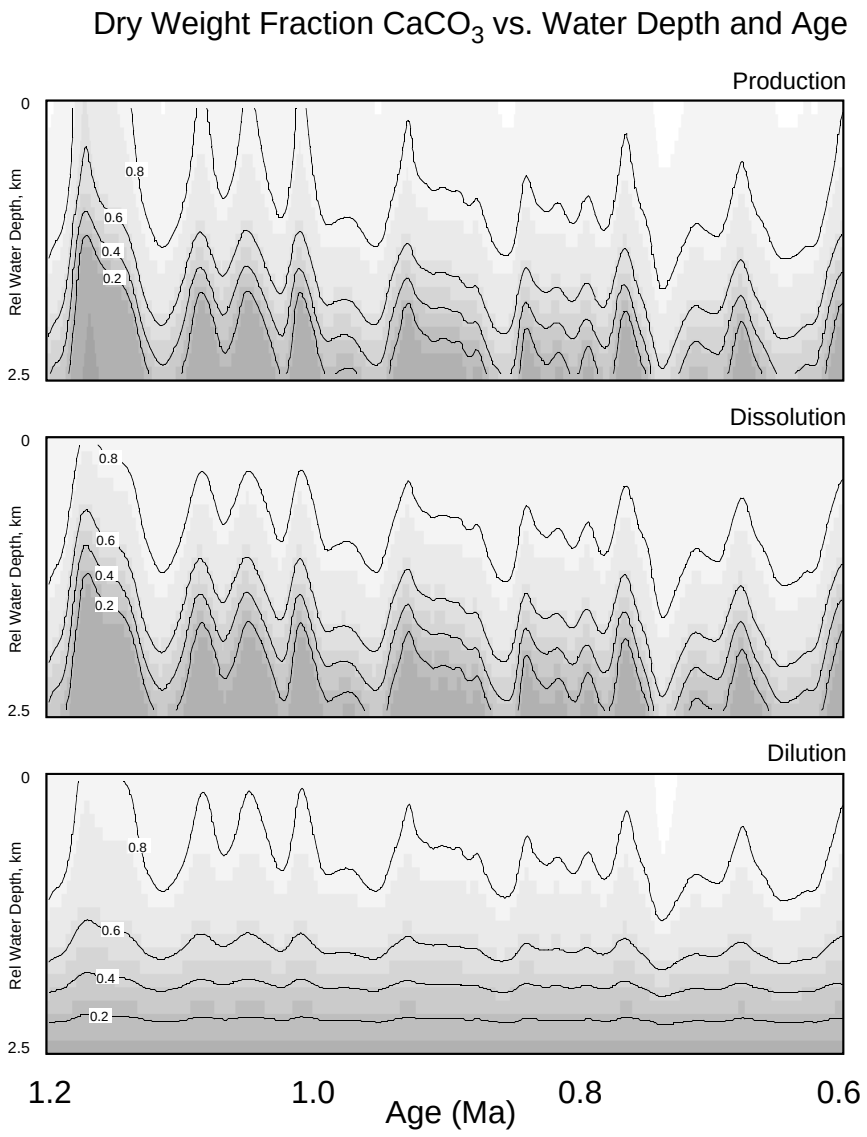


Figure 8. Equilibrium calcite burial model output of the calculated sedimentary $CaCO_3$ percent "core" records for the Production, Dissolution, and Dilution experiments.

estimate of fractional contribution of NADW at Site 929 it is subject to some error due to slight misalignments between records and resulting differencing errors (Mix et al., 1995). At some levels the Site 929 $\delta^{13}C$ values exceed the $\delta^{13}C$ compositions of the presumed end members, due to either misalignments between records or real basinal $\delta^{13}C$ differences. The calculated fractional $NADW_{929}$ was limited to a range of 0–1; calculated values that exceeded this range were set to the appropriate limit value. The lack of $\delta^{13}C$ data at Site 929 between 0.79 and 0.81 Ma was due to several samples that had very low or absent coarse fractions (scarcity of whole foraminifers). Very low carbonate percentages and high carbonate fragmentation suggest that intense dissolution occurred over this interval, which is consistent with the very low NADW values during this interval at Site 607 in the North Atlantic (41°N; Raymo et al., 1990). Atlantic and Pacific benthic $\delta^{13}C$ values were chemically indistinguishable near 0.8 Ma. Based on new results from equatorial Pacific Site 849, deep Pacific *C. wuellerstorfi* $\delta^{13}C$ data for this interval are heavier than coeval Atlantic $\delta^{13}C$ values (Mix et al., 1995), suggesting a complete shutdown of lower NADW production.

The $NADW_{929}$ record is shown adjacent to Site 929 $\delta^{13}C$, Sites 925, 928, and 929 carbonate accumulation rates, and coarse fraction data in Figure 11. All of the longer duration (>20 k.y.) carbonate flux and coarse fraction minima over the 1.2–0.6 Ma interval coincide with minima in NADW production (shaded intervals; Fig. 11). There is also a close correspondence between the intensity of NADW reduction and the depression of carbonate burial flux and coarse fraction values. Cross-spectral analyses were not attempted with the $NADW_{929}$ record because the associated signal alignment and differencing errors would be expected to sufficiently diminish the temporal resolution as to render phasing or amplitude estimates invalid. As listed in Table 1, benthic $-\delta^{18}O$ and $\delta^{13}C$ at Site 929 are coherent and in-phase at the dominant 100-k.y. and 41-k.y. periods of variation.

## Atlantic Deep Circulation Changes and Global Carbonate Burial

This study establishes a direct link between changes in Atlantic deep circulation and Atlantic carbonate burial/dissolution over this 1.2–0.6 Ma interval, a conclusion that is consistent with earlier studies on Pleistocene Atlantic carbonate sedimentation (Gardner, 1975; Crowley, 1983, 1985; Verardo and McIntyre, 1994; Curry and Lohmann, 1990). Frequency-domain analyses demonstrate that the car-

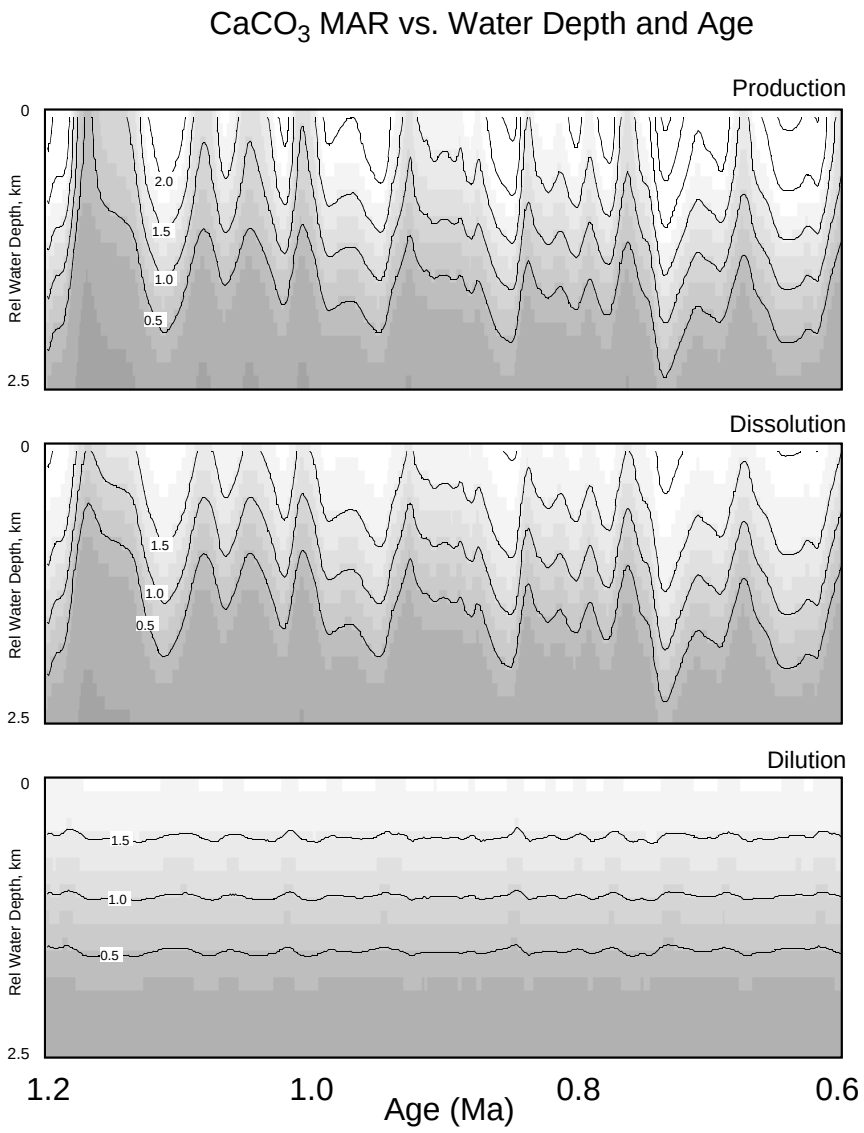


Figure 9. Equilibrium calcite burial model output of the calculated sedimentary carbonate mass accumulation rates (MAR) for the Production, Dissolution, and Dilution experiments.

bonate percentage, burial flux, and coarse fraction records are coherent and in-phase with both benthic $-\delta^{18}O$ and $\delta^{13}C$ at the dominant 100-k.y. and 41-k.y. periodicities, suggesting that glacial dissolution of these carbonate-rich Atlantic sediments due to incursions of corrosive AABW was effectively instantaneous (i.e., no detectable lag at the 95% confidence level). For sediments accumulating under the influence of deep circulation $\Delta CO_3^{=}$ changes, the calcite dissolution model experiments predict that carbonate percent and burial flux records will exhibit specific water-depth-dependent changes in signal amplitude given a series of cores along a bathymetric gradient (Fig. 10). These same changes in carbonate percent and burial flux amplitude are observed in the core data from Sites 925, 928, and 929 (Fig. 6).

In contrast to this Atlantic pattern of carbonate dissolution, carbonate preservation and burial in Pacific and Indian Ocean sediments commonly show significant lags with respect to global ice volume. Farrell and Prell (1989) thoroughly reviewed available Pacific and Indian Ocean carbonate preservation data, noting that most well-dated records from these basins significantly lag global ice volume (as a common chronometer) by an average of one-quarter phase at the primary orbital periodicities. Pacific Ocean carbonate preservation records lag the 100-k.y. component of ice volume by a reported range of 3–20 k.y. (see Farrell and Prell, 1989, for references), whereas the Indian Ocean preservation records lag ice volume by up to 19 k.y. (e.g., Peterson and Prell, 1985).

Based on these results and extant data from other basins, we propose that glacial-interglacial changes in deep Atlantic circulation were primarily responsible for the observed timing and spatial distributions of Pliocene–Pleistocene global carbonate burial cycles. Glacial reductions in NADW production allowed corrosive (low $[CO_3^{=}]$) AABW to advance into the carbonate-rich sediments of the tropical and North Atlantic. Extensive and instantaneous Atlantic carbonate dissolution resulted from the associated rise in Atlantic calcite lysocline levels. Glacial mean ocean alkalinity levels increased in response to this dissolution, and the global ocean net carbonate burial (the amount of calcite which must be buried to balance the continental weathering supply of alkalinity to the ocean) must have increased in the Pacific and Indian Oceans to balance decreases in Atlantic burial fluxes. This was achieved by a deepening of the calcite lysocline in the Pacific and Indian basins in response to increased mean ocean alkalinity levels, which thereby increase oceanic $[CO_3^{=}]$ levels (using $[CO_3^{=}] = [Alk] - [\Sigma CO_2]$; Broecker and Peng, 1982). However, this process of restoring the equilibrium global calcite burial is not instantaneous but, rather, is constrained by the mean response time of

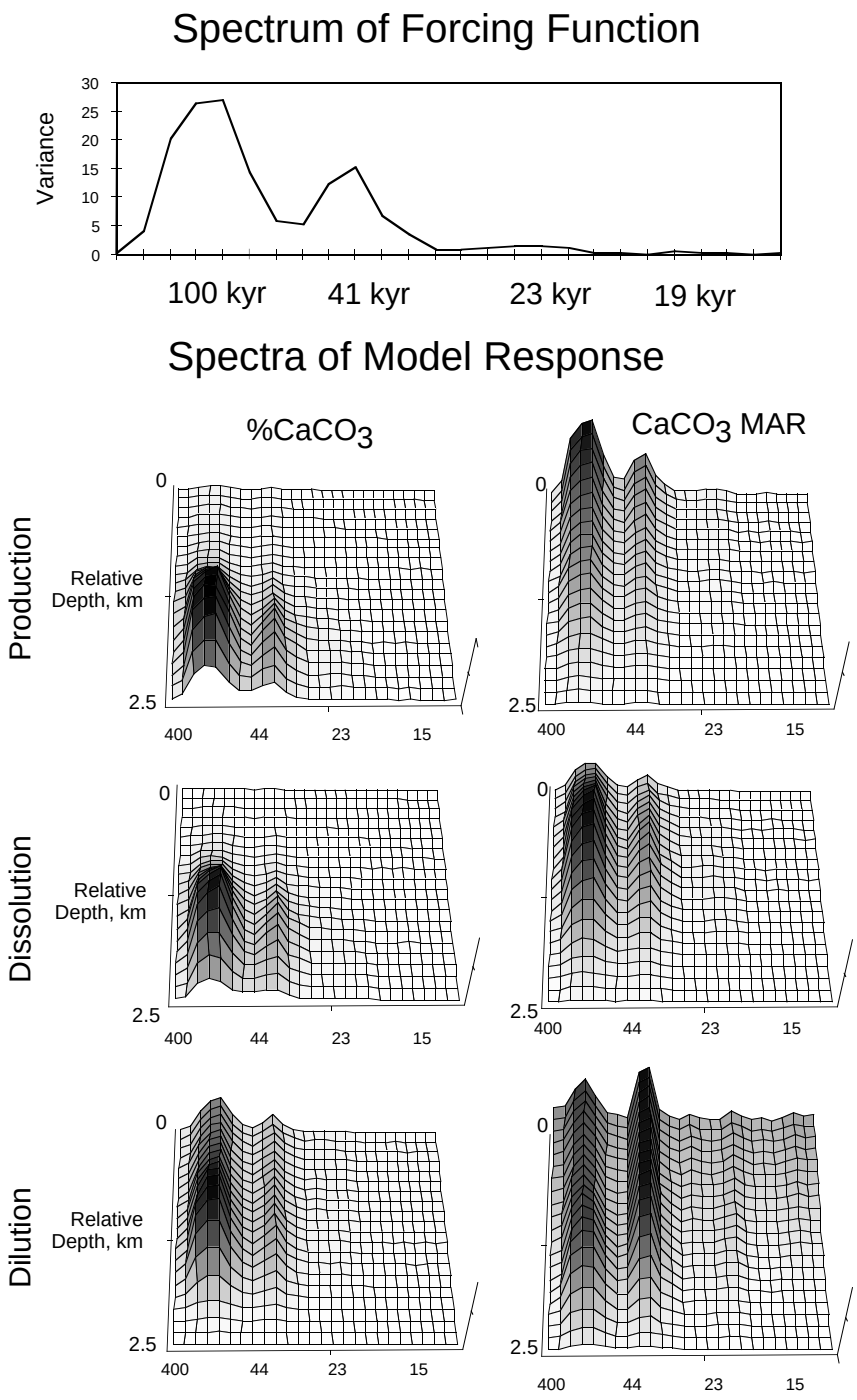


Figure 10. Three-dimensional power spectra (Frequency–Amplitude–Water depth) of the $CaCO_3$ percentage and accumulation rate data calculated for the separate Production, Dissolution, and Dilution experiments. The Production and Dissolution experiments exhibit similar variance characteristics with water depth, which are distinct from the Dilution experiment results.

oceanic [$CO_3^=$], which is estimated near 5–15 k.y. (Broecker and Peng, 1982; Broecker, 1971; Boyle, 1988). Hence, instantaneous dissolution of Atlantic carbonate sediments is compensated by net carbonate burial in the Pacific and Indian Basins.

The primary lines of evidence that support this view are:

1. Strong, in-phase covariation between benthic $-\delta^{18}O$ and $\delta^{13}C$ are examples of changes in deep Atlantic circulation that are linked to glacial-interglacial climate change with no appreciable phase lag.
2. Strong, in-phase covariation of these records with changes in Atlantic carbonate burial are examples of Atlantic carbonate dissolution that responds rapidly, with no appreciable phase lag, to changes in Atlantic deep circulation.
3. Atlantic and Atlantic-sector Southern Ocean sediments comprise >50% of the global mean carbonate burial (Milliman, 1993) and are thus an important component of the mean ocean carbonate burial sink.
4. Pacific and Indian Ocean carbonate preservation and burial records are out of phase with Atlantic records and significantly lag the common $\delta^{18}O$ ice volume chronometer at the primary orbital periodicities.
5. The Pacific and Indian Ocean carbonate lag durations are roughly equivalent to the mean response time of global ocean carbonate ion concentrations (~5–15 k.y.).

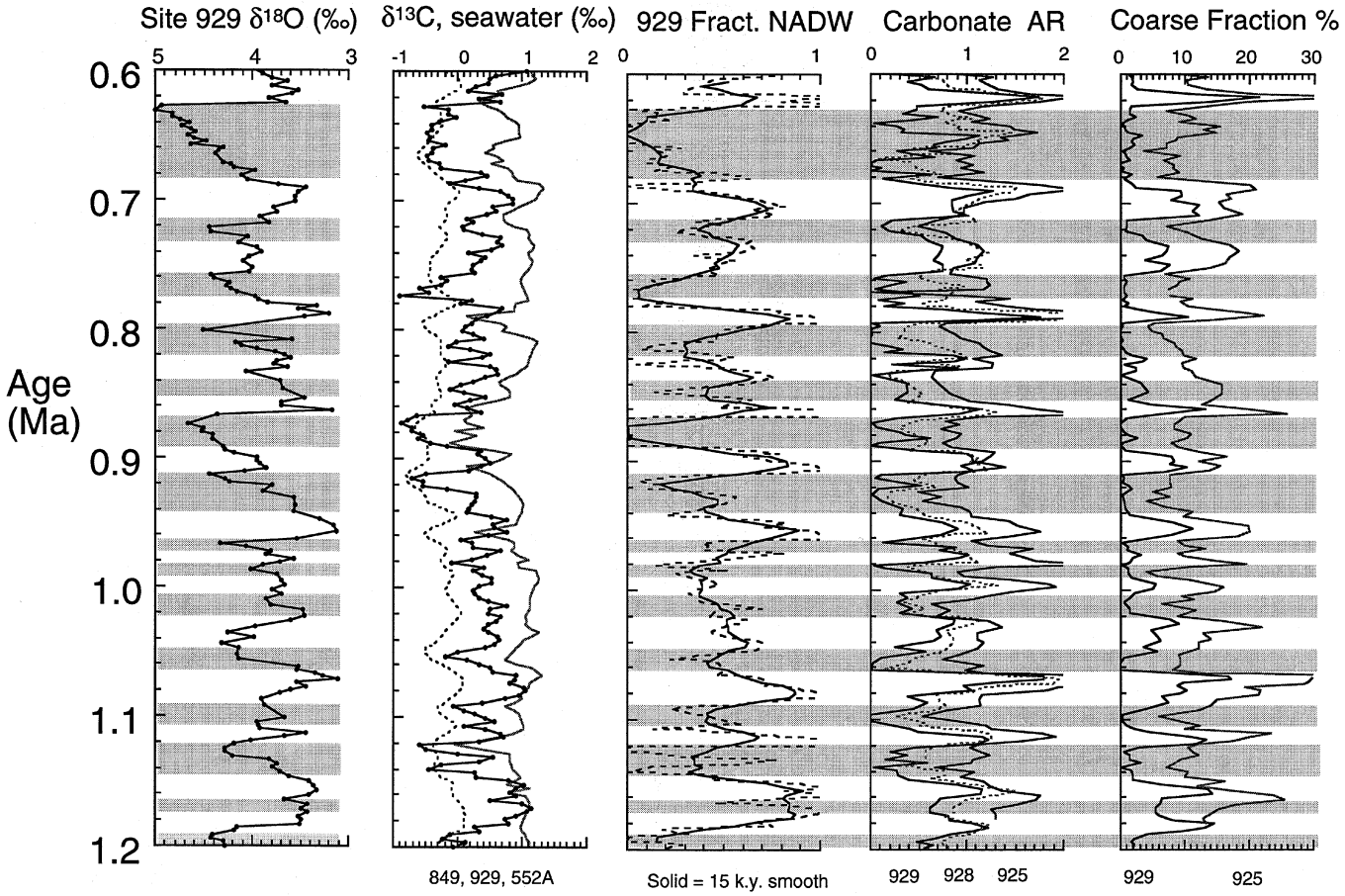


Figure 11. Fractional variations in NADW composition of bottom water calculated for Site 929 on the Ceara Rise compared to carbonate accumulation rate and coarse fraction (>64 µm) data from Sites 925, 928, and 929. Note the strong correspondence between apparent reductions in NADW at Site 929 and the reduced carbonate burial fluxes and coarse fraction abundances.

## ACKNOWLEDGMENTS

Careful reviews by Mitch Lyle and David Murray and additional input from Rachel Oxburgh greatly improved the final manuscript. Assistance with benthic foraminifer identification and picking was provided by Mimi Katz and Linda Baker.

### REFERENCES

Archer, D., 1989. Dissolution of calcite in deep-sea sediments: pH and $O_2$ microelectrode results. *Geochim. Cosmochim. Acta,* 53:2831–2845.

Archer, D.E., 1991. Modeling the calcite lysocline. *J. Geophys. Res.,* 96:17037–17050.

Balsam, W.L., 1983. Carbonate dissolution on the Muir Seamount (western North Atlantic): interglacial/glacial changes. *J. Sediment. Petrol.,* 53:719–731.

Blackman, R.B., and Tukey, J.W., 1958. *The Measurement of Power Spectra from the Point of Communications Engineering:* Mineok, NY (Dover).

Boyle, E.A., 1988. Vertical ocean nutrient fractionation and glacial/interglacial $CO_2$ cycles. *Nature,* 331:55–56.

Boyle, E.A., and Keigwin, L.D., 1982. Deep circulation of the North Atlantic over the last 200,000 years: geochemical evidence. *Science,* 218:784–787.

————, 1987. North Atlantic thermohaline circulation during the past 20,000 years linked to high-latitude surface temperature. *Nature,* 330:35–40.

Broecker, W.S., 1971. Calcite accumulation rates and glacial to interglacial changes in oceanic mixing. *In* Turekian, K.K. (Ed.), *The Late Cenozoic Glacial Ages:* New Haven, CT (Yale Univ. Press), 239–265.

Broecker, W.S., and Peng, T.H., 1982. *Tracers in the Sea:* Palisades, NY (Eldigio Press).

Broecker, W.S., and Takahashi, T., 1978. The relationship between lysocline depth and in-situ carbonate ion concentration. *Deep-Sea Res. Part A,* 25:65–95.

Charles, C.D., and Fairbanks, R.G., 1992. Evidence from Southern Ocean sediments for the effect of North Atlantic deep-water flux on climate. *Nature,* 355:416–419.

CLIMAP Project Members, 1981. Seasonal reconstructions of the Earth's surface at the last glacial maximum. *Geol. Soc. Am., Map and Chart Ser.,* MC36.

Crowley, T.J., 1983. Calcium carbonate preservation patterns in the central North Atlantic during the last 150,000 years. *Mar. Geol.,* 51:1–14.

————, 1985. Late Quaternary carbonate changes in the North Atlantic and Atlantic/Pacific comparisons. *In* Sundquist, E.T., and Broecker, W.S. (Eds.), *The Carbon Cycle and Atmospheric $CO_2$: Natural Variations, Archean to Present.* Geophys. Monogr., Am. Geophys. Union, 32:271–284.

Curry, W.B., 1996. Late Quaternary deep circulation in the western equatorial Atlantic. *In* Wefer, G., Berger, W.H., Siedler, G. (Eds.), *The South Atlantic: Present and Past Circulation:* Berlin (Springer), 577–598.

Curry, W.B., Duplessy, J.-C., Labeyrie, L.D., and Shackleton, N.J., 1988. Changes in the distribution of $\delta^{13}C$ of deep water $\Sigma CO_2$ between the last glaciation and the Holocene. *Paleoceanography,* 3:317–341.

Curry, W.B., and Lohmann, G.P., 1986. Late Quaternary carbonate sedimentation at the Sierra Leone Rise (eastern equatorial Atlantic Ocean). *Mar. Geol.,* 70:223–250.

————, 1990. Reconstructing past particle fluxes in the tropical Atlantic Ocean. *Paleoceanography,* 5:487–505.

Curry, W.B., Shackleton, N.J., and Richter, C., et al., 1995. *Proc. ODP, Init. Repts.,* 154: College Station, TX (Ocean Drilling Program).

deMenocal, P.B., Oppo, D.W., Fairbanks, R.G., and Prell, W.L., 1992. Pleistocene $\delta^{13}C$ variability of North Atlantic intermediate water. *Paleoceanography,* 7:229–250.

Duplessy, J.-C., Shackleton, N.J., Fairbanks, R.G., Labeyrie, L.D., Oppo, D., and Kallel, N., 1988. Deepwater source variations during the last climatic cycle and their impact on the global deepwater circulation. *Paleoceanography,* 3:343–360.

Duplessy, J.-C., Shackleton, N.J., Matthews, R.K., Prell, W.L., Ruddiman, W.F., Caralp, M., and Hendy, C., 1984. $^{13}C$ record of benthic foraminifera in the last interglacial ocean: implications for the carbon cycle and the global deep water circulation. *Quat. Res.,* 21:225–243.

Emerson, S., and Archer, D., 1992. Glacial carbonate dissolution cycles and atmospheric $pCO_2$: a view from the ocean bottom. *Paleoceanography,* 7:319–331.

Farrell, J., and Prell, W.L., 1989. Climatic change and $CaCO_3$ preservation: an 800,000-year bathymetric reconstruction from the central equatorial Pacific Ocean. *Paleoceanography,* 4:447–466.

Gardner, J.V., 1975. Late Pleistocene carbonate dissolution cycles in the eastern equatorial Atlantic. *In* Sliter, W.V., Bé, A.W.H., and Berger, W.H. (Eds.), *Dissolution of Deep-Sea Carbonates.* Spec. Publ. Cushman Found. Foraminiferal Res., 13:129–141.

Gill, A.E., 1982. *Atmosphere-Ocean Dynamics:* New York (Academic).

Imbrie, J., Berger, A., Boyle, E., Clemens, S., Duffy, A., Howard, W., Kukla, G., Kutzbach, J., Martinson, D., McIntyre, A., Mix, A., Molfino, B., Morley, J., Peterson, L., Pisias, N., Prell, W., Raymo, M., Shackleton, N., and Toggweiler, J., 1993. On the structure and origin of major glaciation cycles, 2. The 100,000-year cycle. *Paleoceanography*, 8:699–735.

Keigwin, L.D., and Lehmann, S.J., 1994. Deep circulation change linked to Heinrich Event 1 and Younger Dryas in a middepth North Atlantic core. *Paleoceanography,* 9:185–194.

Kroopnick, P., 1985. The distribution of $^{13}C$ of $\Sigma CO_2$ in the world oceans. *Deep-Sea Res. Part A,* 32:57–84.

Milliman, J.D., 1993. Production and accumulation of calcium carbonate in the ocean: Budget of a non-steady state. *Global Biogeochem. Cycles,* 7:927–957.

Mix, A.C., Pisias, N.G., Rugh, W., Wilson, J., Morey, A., and Hagelberg, T.K., 1995. Benthic foraminiferal stable isotope record from Site 849: 0–5 Ma: local and global climate changes. *In* Pisias, N.G., Mayer, L.A., Janecek, T.R., Palmer-Julson, A., and van Andel, T.H. (Eds.), *Proc. ODP, Sci. Results,* 138: College Station, TX (Ocean Drilling Program), 371–412.

Oppo, D.W., and Fairbanks, R.G., 1987. Variability in the deep and intermediate water circulation of the Atlantic Ocean during the past 25,000 years: Northern Hemisphere modulation of the Southern Ocean. *Earth Planet. Sci. Lett.,* 86:1–15.

————, 1990. Atlantic Ocean thermohaline circulation of the last 150,000 years: Relationship to climate and atmospheric $CO_2$. *Paleoceanography,* 5:277–288.

Oppo, D.W., and Lehman, S.J., 1993. Mid-depth circulation of the subpolar North Atlantic during the last glacial maximum. *Science,* 259:1148–1152.

Oppo, D.W., Raymo, M.E., Lohmann, G.P., Mix, A.C., Wright, J.D., and Prell, W.L., 1995. A $\delta^{13}C$ record of upper North Atlantic deep water during the past 2.6 million years. *Paleoceanography,* 10:373–394.

Peterson, L.C., and Prell, W.L., 1985. Carbonate preservation and rates of climatic change: an 800 kyr record from the Indian Ocean. *In* Sundquist, E.T., and Broecker, W.S. (Eds.), *The Carbon Cycle and Atmospheric $CO_2$: Natural Variations, Archean to Present.* Geophys. Monogr., Am. Geophys. Union, 32:251–270.

Rahmsdorf, S., 1995. Bifurcations of the Atlantic thermohaline circulation in response to changes in the hydrological cycle. *Nature,* 378:145–150.

Raymo, M.E., Ruddiman, W.F., Shackleton, N.J., and Oppo, D.W., 1990. Evolution of Atlantic-Pacific $\delta^{13}C$ gradients over the last 2.5 m.y. *Earth Planet. Sci. Lett.,* 97:353–368.

Ruddiman, W.F., Shackleton, N.J., and McIntyre, A., 1986. North Atlantic sea-surface temperatures for the last 1.1 million years. *In* Summerhayes, C.P., and Shackleton, N.J. (Eds.), *North Atlantic Paleoceanography:* London (Geological Society of London), 155–173.

Shackleton, N.J., 1974. Attainment of isotopic equilibrium between ocean water and the benthonic foraminifera genus *Uvigerina:* isotopic changes in the ocean during the last glacial. *Les Meth. Quant. d'etude Var. Clim. au Cours du Pleist., Coll. Int. C.N.R.S.,* 219:203–209.

Shackleton, N.J., Backman, J., Zimmerman, H., Kent, D.V., Hall, M.A., Roberts, D.G., Schnitker, D., Baldauf, J.G., Desprairies, A., Homrighausen, R., Huddlestun, P., Keene, J.B., Kaltenback, A.J., Krumsiek, K.A.O., Morton, A.C., Murray, J.W., and Westberg-Smith, J., 1984. Oxygen isotope calibration of the onset of ice-rafting and history of glaciation in the North Atlantic region. *Nature,* 307:620–623.

Verardo, D.J., and McIntyre, A., 1994. Production and destruction: control of biogenous sedimentation in the tropical Atlantic 0–300,000 years B.P. *Paleoceanography,* 9:63–86.

**Date of initial receipt: 5 December 1995**
**Date of acceptance: 19 August 1996**
**Ms 154SR-113**